Rupture Properties of Blood Vessel Walls Measured by Pressure-Imposed Test*

Toshiro OHASHI**, Syukei SUGITA**, Takeo MATSUMOTO**,***,
Kiichiro KUMAGAI****, Hiroji AKIMOTO****,
Koichi TABAYASHI**** and Masaaki SATO**

It is expected to be clinically useful to know the mechanical properties of human aortic aneurysms in assessing the potential for aneurysm rupture. For this purpose, a newly designed experimental setup was fabricated to measure the rupture properties of blood vessel walls. A square specimen of porcine thoracic aortas is inflated by air pressure at a rate of 10 mmHg/s (≈1.3 MPa/s) until rupture occurs. Mean breaking stress was 1.8±0.4 MPa (mean±SD) for the specimens proximal to the heart and 2.3±0.8 MPa for the distal specimens, which are not significantly different to those values obtained longitudinally from conventional tensile tests. Moreover, the local breaking stretch ratio in the longitudinal direction was significantly higher at the ruptured site (2.7±0.5) than at the unruptured site (2.2±0.4). This testing system for studying the rupture properties of aortic walls is expected to be applicable to aortic aneurysms. Experimental verification of the present technique for the homogeneous, isotropic material is also presented.

Key Words: Biomechanics, Measurement, Fracture Mechanics, Breaking Stress, Thoracic Aortas, Pressure-Imposed Tests

1. Introduction

Aortic aneurysm is a crucial disease because its diameter may increase until rupture occurs and this usually has fatal consequences. Despite tremendous advances in surgical techniques, the mortality of ruptured aneurysm is more than 97%[1]. At present, in large institutions a thoracic aortic aneurysm is replaced with aortic prostheses when its maximal diameter exceeds about 5 cm, in order to avoid rupture[2]. However, some aneurysms rupture at a diameter smaller than 5 cm[3]. This empirical knowledge such as a diameter is not a sufficient criterion. Therefore, a reliable predictor is necessary in assessing the potential for aneurysm rupture.

An association between aortic aneurysm formation and generalized atherosclerotic disease has long been indicated, and the major risk factors for atheroscretotic disease are high blood pressure, high-serum lipid, smoking, and low insulin levels. From a biomechanical point of view, some correlation may exist between aortic aneurysm rupture and the mechanical properties of the aneurysm. Changes in mechanical properties may be of great importance in aneurysm formation, where a degenerative change in the blood vessel walls leads to dilation and rupture. Although the mechanical properties of blood vessel walls have been studied extensively, those of aortic aneurysm are still not well known due to difficulties in obtaining and handling human aneurysm specimens.

In previous studies, Sterpetti et al.[4] reported that the ratio of aneurysm diameter to vessel diameter was a more effective risk factors for aneurysm rupture than aneurysm diameter alone. Wilson et al.[5] hypothesized that aortic compliance might provide a more

* Received 24th June, 2002 (No. 02-4122)
** Graduate School of Engineering, Tohoku University, 01 Aoba-yama, Sendai, Miyagi 980-8579, Japan. E-mail: ohashi@biomech.mech.tohoku.ac.jp
*** Department of Mechanical Engineering, Nagoya Institute of Technology "Omohi" College, Nagoya, Japan
**** Graduate School of Medicine, Tohoku University, Sendai, Japan

precise quantification of risk factors for aneurysm rupture and showed that a ruptured abdominal aortic aneurysm was significantly lower in the pressure-strain elastic modulus than an unruptured aneurysm, observed using ultrasonography. MacSweeney et al.[6] also measured the pressure-strain elastic modulus of aneurysmal aorta and showed that inelasticity of aneurysmal vessels was attributable to the loss of elasticity. However, these variables were obtained only on the basis of changes in the aneurysm geometries before rupture. Although Raghavan et al.[7] performed uniaxial tensile testing on a human aneurysmal aorta to determine the ultimate strength, and indicated that aneurysm rupture might be related to a reduction in the tensile strength, the uniaxial tensile testing has difficulty in cutting a specimen out from the aneurysm and providing only uniaxial properties (not biaxial properties). Since blood vessel walls are subjected to hemodynamic stresses, rupture properties should be evaluated by a pressure-imposed test from a physiological standpoint.

In the present study, we fabricated an experimental setup for pressure-imposed tests in order to measure the rupture properties of thoracic aortic aneurysms. The experimental setup was newly designed to rupture rectangular specimens excised from aneurysms. As the first step, we applied this technique to the rupture tests of porcine descending thoracic aortas. The results obtained using this technique were compared with those obtained from conventional uniaxial tensile tests. Our final goal should be to measure the rupture properties of human aortic aneurysms, which would be an important advancement toward the estimation of rupture potential of aneurysms.

2. Materials and Methods

2.1 Design of apparatus

Most aneurysm specimens which can be obtained in hospitals are not tubular specimens but rectangular specimens. Therefore, we designed an experimental setup which can apply pressure to rectangular specimens. The pressure is applied not by water but by air for simplicity in manipulation. A detailed view of the experimental setup for specimen mounting is shown schematically in Fig. 1. The setup mainly consists of a rubber balloon and three metal plates with a hole (top, middle, and bottom plates). The specimen is mounted on the middle plate with the hole of 20 mm in diameter, with its adventitial side to be measured facing up. The adventitial surface of the specimen is marked with black ink in the circumferential and longitudinal directions at 2 mm intervals. These dots are used as a reference in measuring the local stretch ratio. The rubber balloon on the bottom plate is used to apply pressure to the specimen. The specimen deforms through the hole of the top plate which is 15 mm in diameter. After mounting the specimen, all the plates are fixed by using eight bolts and are covered with an acryl box to prevent fragments of broken specimens from falling on the floor.

A schematic diagram of the pressure-imposed tests is shown in Fig. 2. Air pressure to inflate the rubber balloon is generated by an air compressor (DSP-02P, Iwata, Japan) and transferred to an electropneumatic regulator (ITV2050-212 BL5, SMC, Japan) via an air filter (AF2000, SMC, Japan). The applied pressure is measured with a pressure transducer (PGM-5KC, Kyowa, Japan) and transferred to a personal computer (DynaBOOK, TOSHIBA, Japan) via a strain amplifier (AS1201, NEC San-ei Instruments, Japan). The security finger valve against pressure overload is rendered dysfunctional. The experiments are controlled by the personal computer which runs a data acquisition software (LabVIEW5.0, National Instruments, Japan). The deformation process of the specimen surface is observed on a TV monitor screen (TM1550, Ikegami, Japan) through

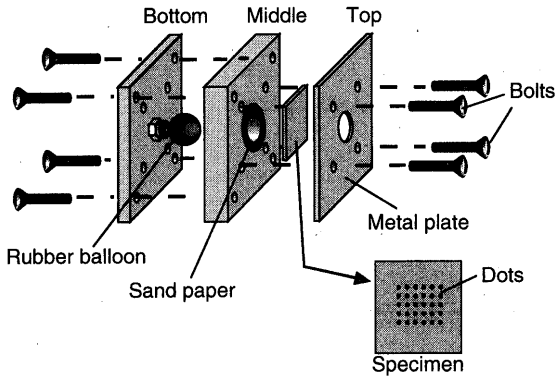

Fig. 1 Experimental setup of specimen mounting

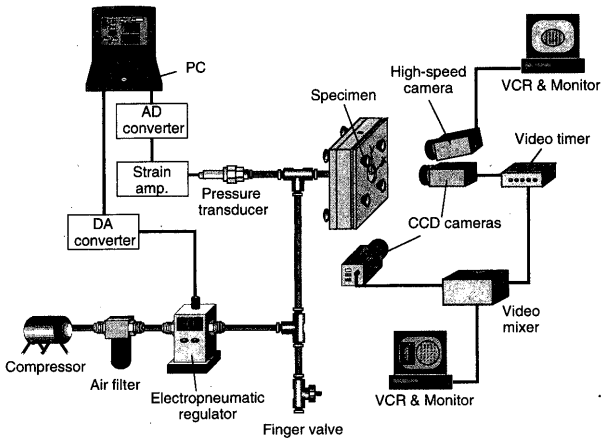

Fig. 2 Schematic diagram of pressure-imposed tests

one CCD camera (CS3150, Tokyo Electronics, Japan) for the front view and another CCD camera (TM1650, TOSHIBA, Japan) for the side view. The two images are superimposed on the TV monitor screen through a digital video mixer (MX-1, VIDEONICS, Japan), and are continuously recorded by a VCR (HR-TS1, Victor, Japan) with a video timer (VTG-33, FOR-A, Japan) with increasing the applied pressure. Furthermore, a high-speed camera (FIRSTCAM-Net 1000/Max, Fotoron, Japan) is used for the detailed observation of the rupture site.

2.2 Specimen preparation and experimental protocol

Six porcine descending thoracic aortas (see Fig. 3, approx. 20 mm in outer diameter, 2 mm in thickness) were obtained just after death at a local slaughterhouse. The thoracic aortas were immediately immersed in physiological saline solution, transported to the laboratory, and then stored at 4°C until the mechanical testing was performed within 72 hours postmortem. The aortas were trimmed, and the intercostal arteries and the surrounding tissues were carefully removed from the aortas with forceps and scissors. The aortas were then cut longitudinally into flat slabs along the intercostal arteries and square specimens of 20×20 mm were excised from the proximal and the distal regions. The various positions of the specimens along the aortas were identified by referring to the intercostal arteries (IA-1 to IA-6), as shown in Fig. 3. The thickness of each square specimen was measured with an area micrometer of our own design. Each square specimen was then mounted on the experimental setup after marking its adventitial surface with a black ink in the circumferential and longitudinal directions at 2 mm intervals, as previously described. Care was taken not to give the specimen any external load. Air pressure was applied into the rubber balloon to inflate the specimen at a rate of 10 mmHg/s (≈1.3 MPa/s) until rupture occurred (max. 5 000 mmHg (≈665 MPa)). The deformation process was observed through the two CCD cameras and the high-speed camera. Images were recorded every second and analyzed to measure the specimen geometries with a image processing software (NIH Image 1.62, National Institute of Health, USA) on a personal computer (Power Mac G4 Cube, Apple Computer, USA). The rate of the high-speed camera was 3 000 frames/s.

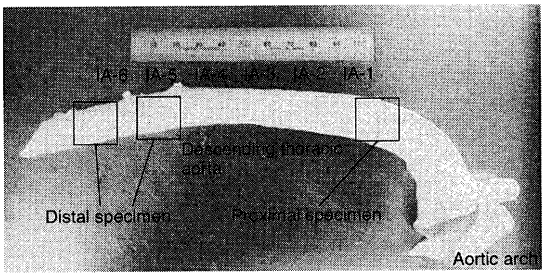

Fig. 3 Schematic diagram to show specimen position along the thoracic aorta. Intercostal arteries are used to identify these positions.

2.3 Characteristic parameters

Mean breaking stress and stretch ratio were estimated from the specimen geometries and the applied pressure under the assumption that the specimen is incompressible and isotropic. In addition, the deformed state is assumed to be a combined geometry of a thin-walled hemisphere and a thin-walled cylinder when rupture occurred. The parameters were calculated as follows.

For a thin-walled hemisphere, the Laplace law leads to:

$$\sigma=\frac{PR}{2T}, \tag{1}$$

where σ is the stress, P the transmural pressure, R the radius of curvature, and T the thickness. The parameter R is identical to the radius of the hole of the top plate in Fig. 1. The parameter T is calculated by the following equation:

$$T=\frac{\pi r^{*2}t^{*}}{S}, \tag{2}$$

where r^{*} is the radius of the hole, r^{*} the initial thickness, and S the area. The specimen area S is expressed as:

$$S=\frac{4\pi r^{*2}}{2}+2\pi R(D_{\max}-R)=2\pi RD_{\max} \tag{3}$$

where $D_{\max}$ is the maximum displacement. By substituting Eqs.(2) and (3) into Eq.(1), the mean stress is found as follows:

$$\sigma=\frac{PD_{\max}}{t^{*}}. \tag{4}$$

The mean stretch ratio is calculated as follows:

$$\lambda=\frac{\pi R+2(D_{\max}-R)}{2R}. \tag{5}$$

The local breaking stretch ratio was also measured from the differences in distance between dots on the specimen surface.

2.4 Tensile test

In a separate experiment, we performed a tensile test on the thoracic aortas using an uniaxial tension tester (AGS-50D, Shimadzu, Japan). A dumbbell-shaped specimen (approx. 40×15×2 mm) with a gauge section length of 10 mm was cut out from the thoracic aortas. The cross-sectional area of the specimen was measured with the area micrometer. Parallel lines with an insoluble ink were marked on the middle of the specimen in order to obtain strain data. The specimen was stretched at a tensile speed

of 20 mm/min, being constantly irrigated with a physiological saline solution. The gauge length was observed on a TV monitor screen (PM-141, Ikegami, Japan) through a CCD camera (TM1650), measured with a video dimension analyzer (C3161, Hamamatsu, Japan) and continuously recorded on an X-Y recorder (WX2400, Graphtech, Japan), along with the corresponding response in load. The stress-strain curve was constructed and the mean breaking stress was calculated. No preconditioning was carried out in the experiments.

2.5 Statistical analysis

Differences and correlations among the data were analyzed using the unpaired Student's t test for equal variance and the unpaired Welch's test for unequal variance, respectively. A value of $p<0.05$ was considered to be significant in all analyses. Data are expressed as mean $\pm$SD.

3. Results

To demonstrate the effectiveness of the present method, an experimental comparison was made for a silicone rubber for the pressure-imposed tests and the uniaxial tensile tests. This material can be considered to be homogeneous and isotropic. The conventional dumbbell-shaped specimen (approx. 40 mm$\times$15 mm $\times$1 mm), with a gauge section width of 6 mm and length of 15 mm, was cut out from the material and subjected to the tensile tests. The stress-strain curve was obtained up to rupture. The breaking stress obtained from the tensile tests (47.0 ± 5.4) was compared with those obtained from the pressure-imposed tests (40.4 ± 4.0). Student's t test proved that the results for these two tests showed no significant difference for this homogeneous, isotropic material ($p<0.05$).

A typical deformed state of the porcine thoracic aortas for (a) the side view and (b) the front view are shown in Fig. 4. We use a Cartesian coordinates system (x, y, z), corresponding with the x, y, and z directions in the circumferential, longitudinal, and radial directions of the blood vessel walls, respectively. The typical photographs of ruptured specimens for (a) the adventitial side and (b) the luminal side are shown in Fig. 5. Rupture occurred parallel to the circumferential direction for all the specimens.

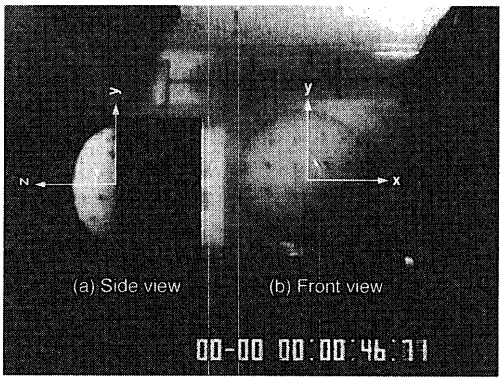

Fig. 4 Typical deformed state of the specimen surface. (a) Side view and (b) front view

The breaking stresses for the specimens proximal and distal to the heart were obtained from the pressure-imposed tests and compared with those obtained from the conventional uniaxial tensile tests, as shown in Fig. 6. In the pressure-diameter tests, the mean breaking stress was 1.8 ± 0.4 MPa for the proximal specimens and 2.3 ± 0.8 MPa for the distal specimens. Comparing the breaking stresses among the proximal specimens and among the distal specimens, no significant differences were found between the pressure-imposed test results and the longitudinal tensile test results (1.5 ± 0.5 for proximal, 2.0 ± 0.7 for distal). In contrast, significant differences were found between the pressure-imposed test results and the circumferential tensile test results (4.0 ± 0.7 for proximal, 3.3 ± 0.6 for distal). In the tensile tests, the breaking stresses were significantly higher in the circumferential direction than in the longitudinal direction for the proximal and distal specimens. For all groups, there were no

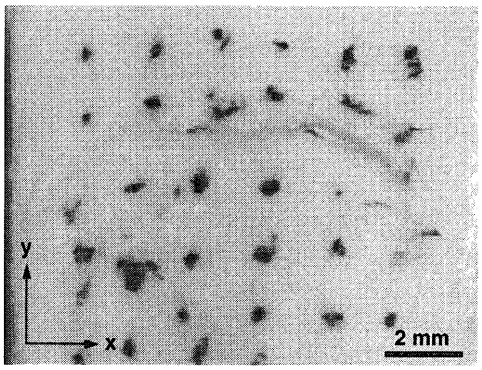

(a) Adventitial side

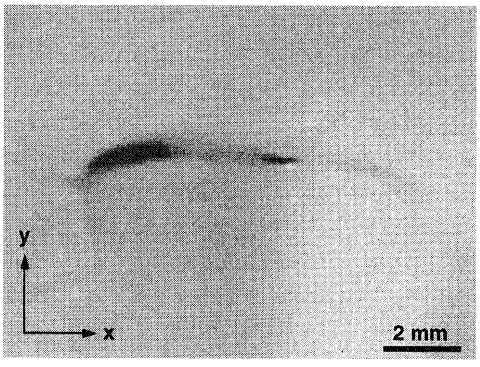

(b) Luminal side

Fig. 5 Typical ruptured specimen for (a) adventitial side and (b) luminal side, showing a tear parallel to the circumferential direction

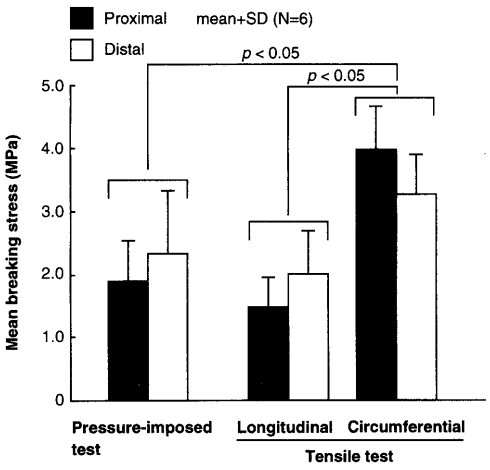

Fig. 6 Comparison of breaking stresses between pressure-imposed tests and uniaxial tensile tests

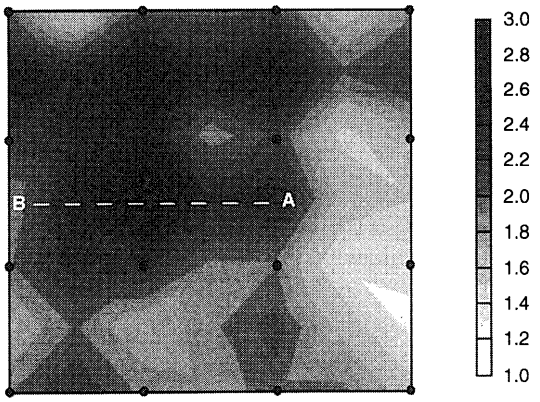

Fig. 7 Distribution of local stretch ratio just before rupture

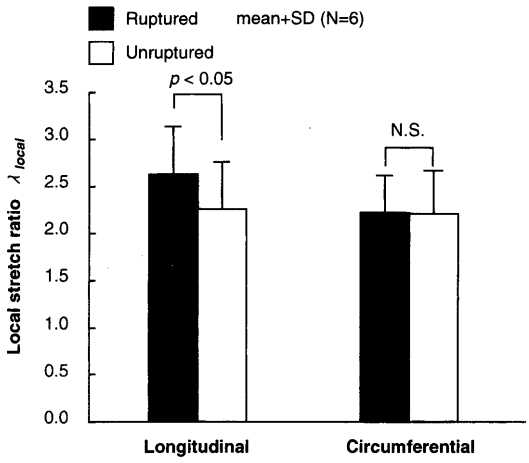

Fig. 8 Local stretch ratios at ruptured and unruptured sites

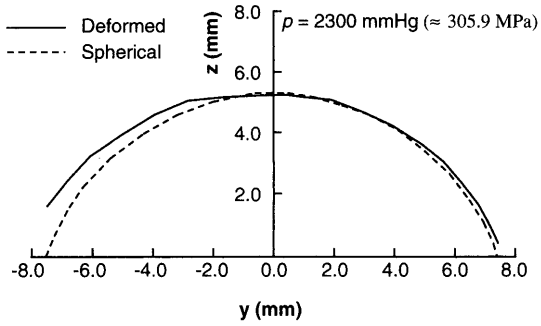

Fig. 9 Comparison of deformed state and spherical curve just before rupture

significant differences in breaking stress between the proximal and distal specimens. In addition, the mean breaking stretch ratio obtained from the pressure-imposed tests showed a significantly higher value for the proximal specimens (2.02 ± 0.04) than for the distal specimens (1.88 ± 0.04) (figure not shown).

Moreover, the starting point of crack propagation was confirmed from the high-speed images and the local breaking stretch ratio was measured for the proximal specimen. Distribution of the typical local stretch ratio just before rupture is shown in Fig. 7. In the figure, the dashed line shows crack propagation from A to B with a higher stretch ratio. The local stretch ratios at both ruptured and unruptured sites were measured from the images and were compared in Fig. 8. The local stretch ratio at the unruptured site was defined as an averaged value of the differences in distance between dots where cracks were not observed. The local stretch ratio in the longitudinal direction was significantly higher at the ruptured site (2.7 ± 0.5) than at the unruptured site (2.2 ± 0.4), while there was no significant difference in the circumferential direction. For the proximal specimens, the averaged value of these local breaking stretch ratios (2.3 ± 0.4) showed no significant difference from the mean breaking stretch ratio (2.02 ± 0.04), which indicated that the degree of anisotropy in porcine thoracic aortas had little effect on the present analysis.

4. Discussion

The experimental setup for the pressure-imposed test was newly designed and fabricated to measure the rupture properties of porcine descending thoracic aortas. To test the accuracy of the assumption that the deformed state is a sphere, a typical deformed geometry in the cross section of the yz-plane just before rupture at 2 300 mmHg ($\approx$305.9 MPa) and the spherical curve are shown in Fig. 9. Solid and broken lines represent the deformed geometry and the spherical curve, respectively. The difference between the two lines is within 5% in the range of ±6.5 mm of the z direction. A similar result was obtained in the cross section of the xz-plane.

In the pressure-imposed tests, rupture of the aortas occurred and crack propagation proceeded along the circumferential direction of the aortas. This

result indicates that the ultimate tensile strength is higher in the circumferential direction than in the longitudinal direction. Thus, in the pressure-imposed tests, rupture will occur in the direction having the smaller ultimate tensile strength, which implies that the pressure-imposed tests would be effective in clarifying the difference in ultimate tensile strength in the in-plane direction. In the uniaxial tensile tests, the breaking stresses in the longitudinal direction were significantly lower than those in the circumferential direction. Taken together, porcine thoracic aortas can be considered to be orthotropic materials and thus the tensile strength in the longitudinal direction is significantly lower than that in the circumferential direction.

In the pressure range near the rupture, collagen fibers, most of which are recruited, are expected to withstand such a high pressure and orient in the circumferential direction. Collagen fibers are known to be approximately 1 000 times stiffer than the other two components, elastic fibers and smooth muscle cells. In a separate study[8], histological observations of porcine thoracic aortas revealed that collagen fibers and smooth muscle cells uniformly dispersed between elastin lamellae and oriented in the circumferential direction. This histological structure may be closely related to the tensile stiffness of the aortas.

Groenink et al.[9] investigated the mean breaking stress of a normal human thoracic aorta using pressure-diameter testing in relation to age and showed that the mean breaking stress was in the range of 4.7 MPa to 0.9 MPa from donors aged 8 to 59 years. Although the pressure-diameter test may provide useful information on the rupture of aortas under close to in vivo conditions, it cannot be applied to rectangular specimens. There was no significant difference in mean breaking stress between the proximal and distal regions in our studies. Purslow[10] performed a tear test on pig descending thoracic aortas along the aortas from just in front of the first intercostal artery to the sixth intercostal artery, and showed that the longitudinal and circumferential ultimate strength increased with distance from the heart. This difference may be due to the difference between the two experimental tests. The pressure-imposed tests provide the tensile properties of the aortas, while the tear tests provide the shearing properties.

Unlike the mean breaking stress, the mean breaking stretch ratio of the proximal specimens was significantly higher than that of the distal specimens. The reason for this difference remains unclear. It is, however, interesting that the standard deviation of the mean breaking stretch ratio is much smaller than that of the mean breaking stress. Therefore, the mean breaking stretch ratio may have a critical value of rupture and it may be of clinical value to estimate the functional state of the aortas in aortic degenerative. It is also interesting that local stretch ratios were significantly different between ruptured and unruptured sites. Further study is necessary to understand the mechanism of rupture on the basis of the mechanical parameters together with the wall microstructure.

There are several limitations to this study that should be noted. One of the limitations is that, in the specimen preparation, cylindrical specimens are cut longitudinally into flat slabs while rectangular specimens are examined. This geometrical difference may affect the breaking properties of the aortas. Another limitation is that since the degree of anisotropy of porcine thoracic aortas is small, the deformation could be assumed to be a spherical shape. However, the present analysis cannot be applied to the case that the specimens exhibit strong anisotropic properties. Moreover, the deformed geometry of the specimen was assumed to be a thin-walled hemisphere. Just before rupture, the thickness of the porcine aortas was about 1 mm and the ratio of radius to wall thickness was about 7.5. Since the ratio of 10 is generally said to be a criterion for assuming a thin-walled hemisphere in a textbook, the specimen should be assumed to be a thick-walled hemisphere for more accurate analysis. It is our next step to overcome these shortcomings in the future study.

5. Conclusions

We have designed and fabricated the experimental setup for pressure-imposed tests to measure the rupture properties of thoracic aortic aneurysms. As the first step, this technique was applied to porcine thoracic aortas to measure the breaking stress and stretch ratio. The mean breaking stress was 1.8 ± 0.4 MPa for the proximal specimens and 2.3 ± 0.8 MPa for the distal specimens, which showed no significant differences compared with those longitudinally obtained from the conventional tensile tests. Moreover, the local stretch ratio in the longitudinal direction was significantly higher at the ruptured site (2.7 ± 0.5) than at the unruptured site (2.2 ± 0.4). This testing system for studying the rupture properties of aortic walls is expected to be applicable to aortic aneurysms.

Acknowledgments

This work was supported financially in part by Grants-in-Aid for Scientific Research from the Ministry of Education, Culture, Sports, Science and Technology in Japan (Nos. 10480241, 11680834).

References

(1) Johansson, G., Markstrom, U. and Swedenborg, J., Ruptured Thoracic Aneurysms: A Study of Incidence and Mortality Rates, J. Vasc. Surg., Vol. 21, No. 6 (1995), pp. 985-988.

(2) Powell, J.T., Mortality Results for Randomised Controlled Trial of Early Elective Surgery or Ultrasonographic Surveillance for Small Abdominal Aortic Aneurysms, The Lancet, Vol. 352 (1998), pp. 1649-1655.

(3) Darling, R.C., Messina, C.R., Brewster, D.C. and Ottinger, L.W., Autopsy Study of Unoperated Abdominal Aortic Aneurysms: The Case for Early Resection, Circulation, Vol. 56 (1977), pp. 161-164.

(4) Sterpetti, A.V., Schultz, R.D., Feldhaus, R.J., Cheng, S.E. and Peetz, D.J., Jr., Factors Influencing Enlargement Rate of Small Abdominal Aortic Aneurysms, J. Surg. Res., Vol. 43, No. 3 (1987), pp. 211-219.

(5) Wilson, K., Bradbury, A., Whyman, M., Hoskins, P., Lee, A., Fowkes, G., McCollum, P. and Ruckley, C.V., Relationship between Abdominal Aortic Aneurysm Wall Compliance and Clinical Outcome: A Preliminary Analysis, Eur. J. Vasc. Endovasc. Surg., Vol. 15 (1998), pp. 472-477.

(6) MacSweeney, S.T.R., Young, G., Greenhalgh, R.M. and Powell, J.T., Mechanical Properties of the Aneurysmal Aorta, Br. J. Surg., Vol. 79 (1992), pp. 1281-1284.

(7) Raghavan, M.L., Webster, M.W. and Vorp, D.A., Ex vivo Biomechanical Behavior of Abdominal Aortic Aneurysm: Assessment Using a New Mathematical Model, Ann. Biomed. Eng., Vol. 24 (1996), pp. 573-582.

(8) Ohashi, T., Kato, Y., Matsumoto, T. and Sato, M., Intramural Distribution of Elastic Moduli in Thoracic Aortas and Its Relation to Histology: Comparison between Porcine and Bovine Thoracic Aortas, JSME Int. J., Ser. C, Vol. 42, No. 3 (1999), pp. 568-573.

(9) Groenink, M., Langerak, S.E., Vanbavel, E., van der Wall, E.E., Mulder, B.J., van der Wal, A.C. and Spaan, J.A., The Influence of Aging and Aortic Stiffness on Permanent Dilation and Breaking Stress of the Thoracic Descending Aorta, Cardiovasc. Res., Vol. 43 (1999), pp. 471-480.

(10) Purslow, P.P., Positional Variations in Fracture Toughness, Stiffness and Strength of Descending Thoracic Pig Aorta, J. Biomech., Vol. 16, No. 11 (1983), pp. 947-953.